ELSEVIER

Journal of Alloys and Compounds 218 (1995) 204–215

Journal of ALLOYS AND COMPOUNDS

Neutron diffraction study of $CeMn_2Ge_2$, $PrMn_2Ge_2$ and $NdMn_2Ge_2$: evidence of dominant antiferromagnetic components within the (001) Mn planes in ferromagnetic $ThCr_2Si_2$-type manganese ternary compounds

R. Welter [a], G. Venturini [a], E. Ressouche [b], B. Malaman [a,*]

[a] *Laboratoire de Chimie du Solide Minéral, Université Henri Poincaré–Nancy I, associé au CNRS (URA 158), BP 239, 54506 Vandoeuvre les Nancy Cédex, France*

[b] *CEA–Département de Recherche Fondamentale sur la Matière Condensée–SPSMS-MDN, 17 rue des Martyrs, 38054 Grenoble Cédex 9, France*

Received 4 August 1994

Abstract

The magnetic properties of $ThCr_2Si_2$-type structure RMn_2Ge_2 (R = Ce, Pr, Nd) compounds have been reinvestigated by the use of neutron diffraction experiments. The ferromagnetic ordering previously proposed to take place on the manganese sublattice is revised. The three compounds are characterized by mixed (001) Mn planes where ferro- and antiferromagnetic components coexist. In the temperature range 2–300 K, $CeMn_2Ge_2$ (T_c = 320 K) exhibits an easy axis conical magnetic structure (cone semiangle $\alpha \approx 60°$) with a total Mn moment value of about 2.7μ_B at 2 K. Ce moments do not order above 1.6 K. At room temperature, $PrMn_2Ge_2$ (T_c = 330 K) and $NdMn_2Ge_2$ (T_c = 330 K) compounds exhibit an easy axis canted ferromagnetic structure ($\phi \approx 60°$) while, at lower temperature ($T < 250$ K), a conical magnetic structure takes place on the Mn sublattice ($\alpha \approx 60°$). The rare earth sublattices orders ferromagnetically below about 100 K. In $PrMn_2Ge_2$, an easy axis prevails in the whole temperature range. At 2 K, the total Mn moment is about 2.8μ_B and the Pr moment value is about 2.9μ_B. On the contrary, in $NdMn_2Ge_2$ the easy axis rotates to the (001) plane below 250 K. At 2 K, the total Mn moment is about 2.7μ_B and the Nd moment value is about 2.3μ_B. In all cases, the thermal dependence of the AF component suggests that an ordering temperature T_N not detected by magnetic moments, occurs at a temperature much higher than the Curie point. The results are compared with those of the related RMnSi, RMnGe and $RMnSi_2$ compounds. The evolution of the magnetic behaviour within the $ThCr_2Si_2$-type structure RMn_2X_2 (X = Si, Ge) compounds is discussed.

Keywords: Neutron diffraction; Antiferromagnetism; Ferromagnetism; Manganese ternary compounds

1. Introduction

The RMn_2Ge_2 (R = rare earths, Ba, Ca) compounds crystallize in the well-known $ThCr_2Si_2$-type structure (space group, *I4/mmm*) [1,2]. These compounds deserve special attention, since their characteristic feature is the presence of long-range ordering of the manganese moments. The magnetic ordering in the manganese sublattice persists up to temperatures higher than 300 K, while the rare earth sublattice orders magnetically at low temperature only. During the last 20 years, the magnetic properties of the RMn_2Ge_2 (R = La–Sm) compounds have been extensively studied by magnetometric and neutron diffraction techniques [3–17]. The main magnetic data are gathered in Table 1.

From bulk magnetization measurements [3,4], it was shown that all these compounds are ferromagnets with Curie temperatures above room temperature (about 306–350 K, Table 1). Furthermore, according to Narasimhan et al. [3], $PrMn_2Ge_2$ and $NdMn_2Ge_2$ exhibit an additional magnetic transition, corresponding to a ferromagnetic ordering of the rare earth sublattice, at $T_t \approx 40$ K while several researchers reported that $SmMn_2Ge_2$ displays a complex magnetic behaviour when the temperature is decreased [5–11].

On the contrary, single-crystal magnetization measurements have been performed on $LaMn_2Ge_2$ [12], $NdMn_2Ge_2$ [13] and $PrMn_2Ge_2$ [14]. All these workers obtained similar ferromagnetic behaviour with Curie

* Corresponding author.

SSDI 0925-8388(94)01378-0

Table 1
Magnetic data for RMn_2Ge_2 compounds (R = La, Ce, Pr, Nd)

Compound	T_c (K)	T_t (K)	θ_p (K)	μ_{eff} (μ_B)	$\mu_{eff,Mn}$ (μ_B)	M (295 K) (μ_B)	M (120 K) (μ_B)	M (4.2 K) (μ_B)	Ref.
$LaMn_2Ge_2$	310								[3]
	310		270	3.5	3.5			3.1	[12]
	325							2.9	[17]
$CeMn_2Ge_2$	316							3.1	[3]
	320		110	6.3	4.0	1.8		2.6	This work
$PrMn_2Ge_2$	334	40						3.9	[3]
	329	80				2.0	4.0	5.9	[14]
	330	40	260	6.1	3.5	1.9	3.4	3.7	This work
$NdMn_2Ge_2$	334	40						6.0	[3]
	336	250, 100				2.2	4.0	5.7	[13]
	330	215, 40	280	6.0	3.4	2.2	3.9	5.2	This work

In Ref. [3], $H_{app} = 20$ kG; in Refs. [12–14], $H_{app} = 50$ kG; in this work, $H_{app} = 17$ kG.

temperatures in fair agreement with the previous published data (Table 1). Moreover, the thermal dependence of the spontaneous magnetization yields T_t values of about 80 K and 100 K for $PrMn_2Ge_2$ and $NdMn_2Ge_2$ respectively. Furthermore, these studies show clearly that the easy axis of magnetization is along the [001] direction in both $LaMn_2Ge_2$ and $PrMn_2Ge_2$ compounds while $NdMn_2Ge_2$ exhibits an easy axis above 250 K and an easy plane below 180 K. It is noteworthy that this spin flop transition, not previously detected [3,4], has been confirmed by Kawashima et al. [15] from permeability measurements under different hydrostatic pressures. The magnetization at 0 K is estimated to be $3.10\mu_B$, $5.9\mu_B$ and $5.7\mu_B$ per formula unit for $LaMn_2Ge_2$, $PrMn_2Ge_2$ and $NdMn_2Ge_2$ respectively. Assuming a Mn moment of $1.55\mu_B$, as estimated from the data on $LaMn_2Ge_2$ [12], the Pr and Nd moments are deduced to be slightly reduced to $2.77\mu_B$ and $2.60\mu_B$ respectively. Under these conditions, the results have been analysed in terms of the molecular field theory including the crystal field, yielding reasonable agreement with the experimental results.

From neutron diffraction experiments, Leciejewicz et al. [16] concluded that $CeMn_2Ge_2$ is a simple collinear ferromagnet, with planes of Mn moments aligned parallel to the c axis, and that no order occurs on the Ce sublattice. At 4.2 K, $\mu_{Mn} = 1.65(15)\mu_B$, in agreement with the value deduced from magnetization measurements on powder or single-crystal samples (Table 1).

More recently, a neutron diffraction study of the ferromagnetic $LaMn_2Ge_2$ and $LaMn_2Si_2$ compounds [17] has led us to revise the ferromagnetic ordering previously proposed for these compounds. At high temperature, both compounds are purely collinear antiferromagnets (not detected by magnetic measurements), characterized by a stacking of antiferromagnetic (001) Mn planes as observed in the related RMnX (X = Si, Ge) compounds [18,19] or in the isotypic $CaMn_2Ge_2$ and $BaMn_2Ge_2$ compounds [20]. These results have been confirmed by Nowick et al. [21]. From Mössbauer spectroscopy measurements on ^{57}Fe-doped $RMn_2Si_{2-x}Ge_x$ compounds, these researchers inferred T_N values of about 420 K and 470 K for $LaMn_2Ge_2$ and $LaMn_2Si_2$ respectively. Below T_c, both compounds exhibit an easy-axis ferromagnetic behaviour. However, the occurrence of a dominant antiferromagnetic component within the (001) Mn planes yields a conical magnetic structure for the germanide (cone semiangle $\alpha \approx 58°$) and a canted magnetic structure for the silicide ($\phi \approx 49°$) (see Figs. 4 and 7 of Ref. [17]). At 2 K, the total Mn moment is about $3.0\mu_B$ and $2.4\mu_B$ for $LaMn_2Ge_2$ and $LaMn_2Si_2$ respectively, values largely higher than that commonly assumed (see above).

According to these results, it is rather surprising that $CeMn_2Ge_2$ does not behave similarly since the nuclear magnetic resonance (NMR) studies undertaken by Sampathkumaran et al. [22] lead to the same hyperfine fields for both $CeMn_2Ge_2$ and $LaMn_2Ge_2$.

Moreover, from neutron diffraction studies on the structurally related CeFeSi-type equiatomic rare earth manganese silicides and germanides RMnX [18,19], we found that compounds with Mn–Mn intralayer distances d_{ip} greater than about 2.85 Å were characterized by antiferromagnetic Mn layers. This criterion is fulfilled within the $ThCr_2Si_2$ silicides (at least at high temperature), where $LaMn_2Si_2$ [17] ($d_{ip} = 2.91$ Å) exhibits antiferromagnetic Mn planes while $CeMn_2Si_2$ [23] ($d_{ip} = 2.85$ Å) and Pr(Nd)Mn_2Si_2 [24] ($d_{ip} = 2.85$ Å) are characterized by ferromagnetic planes, as well as for $CaMn_2Ge_2$, $BaMn_2Ge_2$ and $LaMn_2Ge_2$ [17,20]. Bearing in mind the Mn–Mn intralayer spacings in the RMn_2Ge_2 (R = Ce–Nd) compounds [25], one may conclude that the same phenomenon probably occurs in this series. Indeed, the occurrence of an antiferromagnetic com-

ponent within the (001) Mn layers would explain the surprisingly low values of the Mn moments observed in this series of germanides (Table 1).

Therefore, in order to clarify the magnetic behaviour of the manganese sublattice in this interesting class of compounds, i.e. magnetic arrangement and Mn moment values, we restart a careful magnetic study of $CeMn_2Ge_2$, $PrMn_2Ge_2$ and $NdMn_2Ge_2$ compounds using bulk magnetic measurements and neutron diffraction experiments.

2. Experimental procedures

The compounds were prepared from commercially available high purity elements. Pellets of stoichiometric mixture were compacted using a steel die and then introduced into silica tubes sealed under argon (100 mmHg). First, the samples were heated at 1173 K for preliminary homogenization treatment and then melted in an induction furnace. Purity of the as-cast sample was checked by powder X-ray diffraction technique (Guinier Cu Kα).

The magnetic measurements were carried out on a Faraday balance (between 300 and 800 K) and on a MANICS magnetosusceptometer (between 4.2 and 300 K), in fields up to 1.7 T.

Neutron experiments were carried out at the Siloe Reactor of the Centre d'Etudes Nucléaires de Grenoble. Several patterns have been collected in the temperature range 2–300 K with the one-dimension curved multidetector DN5 at a wavelength $\lambda = 2.4965$ Å. In order to correct texture effects, following a procedure largely described in Ref. [26], we used during the refinements a fitted coefficient f_{cor} which reflects the importance of preferential orientation. The values of f_{cor} obtained (see below) strongly support the validity of this correction.

Using the scattering lengths $b_{Ge} = 8.185$ fm, $b_{Mn} = -3.73$ fm, $b_{Ce} = 4.84$ fm, $b_{Pr} = 4.58$ fm and $b_{Nd} = 7.69$ fm and the form factor of Mn and rare earth elements from Ref. [27] and Ref. [28] respectively, the scaling factor, the atomic positions z_{Ge} and the Mn and rare earth magnetic moments were refined by the mixed crystallographic executive for diffraction (MXD) least-squares fitting procedure [29]. The MXD program allows simultaneous fitting of the nuclear and magnetic intensities to the observed intensities.

In the $ThCr_2Si_2$-type structure (*I4/mmm*), the rare earth and germanium atoms occupy the 2(a) (0,0,0) and 4(e) (0,0, $z \approx 0.38$) sites respectively whereas the Mn atoms occupy the special position 4(d) (0, 1/2, 1/4), i.e. with an additional C translation mode. Thus, it is important to stress that the magnetic contributions to the observed intensities affect only the nuclear lines obeying the limiting reflection conditions: (i) (*hkl*) with $h+k=2n$ for a ferromagnetic ordering of the Mn sublattice; (ii) (*hkl*) with $h+k=2n+1$ for an antiferromagnetic arrangement of the Mn moments within the (001) planes.

In every case, attempts to fit the nuclear lines by interchanging the positions of the Mn and Ge atoms always led to poorer agreement and gave no evidence for any mixing between the Mn and Ge atoms at 4(d) and 4(e) sites as proposed by Sampathkumaran et al. [22].

3. Magnetic measurement

The main characteristic magnetic data are collected in Table 1.

The temperature dependence of the susceptibility ($H_{appl.} = 1.2$ kG) measured in the temperature range 4.2–800 K (Fig. 1) yields Curie temperatures T_c of approximately 320 K, 330 K and 330 K for $CeMn_2Ge_2$, $PrMn_2Ge_2$ and $NdMn_2Ge_2$ respectively. The magnetization value is almost constant for $CeMn_2Ge_2$ in the whole ordering range and increases significantly at low

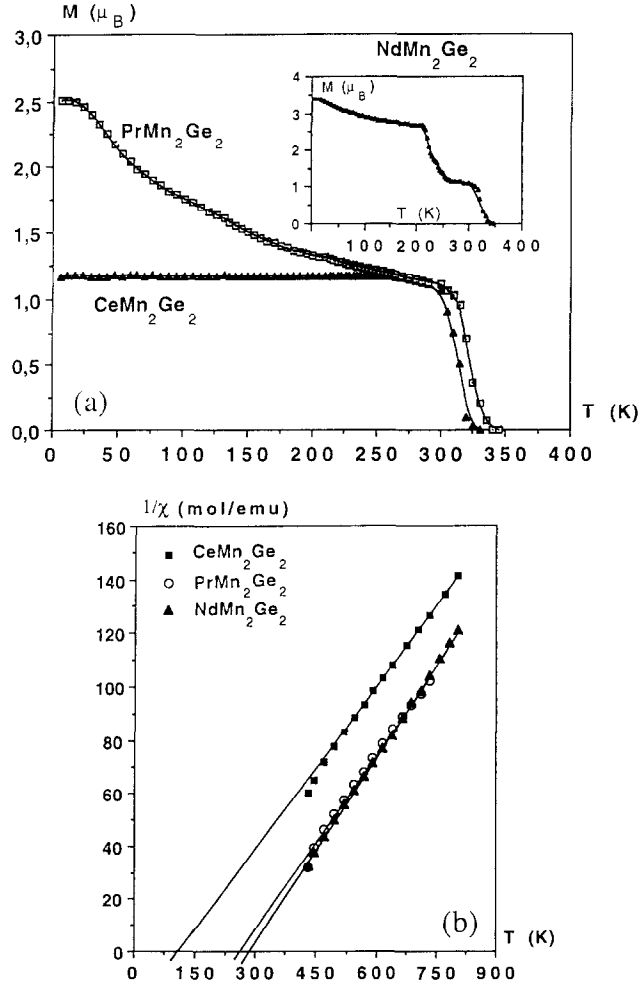

Fig. 1. (a) Temperature dependence of magnetization ($H_{app} = 1200$ G) and (b) inverse of susceptibility ($H_{app} = 5$ kG) in the RMn_2Ge_2 (R = Ce, Pr, Nd) compounds.

temperature (below about 100 K) for $PrMn_2Ge_2$ and $NdMn_2Ge_2$. All these results are in fair agreement with those reported in Refs. [3,4,13,14].

In the case of $NdMn_2Ge_2$, the low field magnetic measurement clearly evidences, between about 250 and 200 K (Fig. 1), the spin flop process pointed out by Shigeoka et al. [12]. Additional measurements show that higher fields smooth this transition which completely vanished under an applied field of about 5 kG. This result probably explains that this transition was not detected by Narashiman et al. [3] who used $H_{appl.} =$ 6 kG.

The maximum magnetization values M_s at 4.2, 120 and 295 K measured under $H_{appl.} = 17$ kG are gathered in Table 1. They are in good accordance with the previous published data [3,4,13,14]. In the case of $PrMn_2Ge_2$, the difference observed between the value obtained on powder samples, $M_s \approx 3.8\mu_B$ (this work and Ref. [3]), and the value obtained on single crystals $M_s \approx 5.9\mu_B$ [14], may probably be related to strong anisotropic effects.

4. Neutron diffraction

Fig. 2 shows the neutron thermograms of the three RMn_2Ge_2 (R = Ce–Nd) compounds recorded between 2 K and 300 K. Depending on temperature, the neutron diffraction patterns are similar to those observed for $LaMn_2Ge_2$ and $LaMn_2Si_2$ respectively (see Section 4 of Ref. [17]) yielding the same magnetic behaviour of the Mn sublattice.

(i) In the whole temperature range for $CeMn_2Ge_2$ and below about 280 K and about 240 K for $PrMn_2Ge_2$ and $NdMn_2Ge_2$ respectively, the thermograms are characterized by the occurrence of several superlattice reflections indexed as satellites of the nuclear lines (*hkl*) with $h + k = 2n + 1$ on the basis of a wavevector $\boldsymbol{k} = 0,0,q_z$). The thermal variation in the Bragg angle values of these lines yields an increase in the q_z values when the temperature decreases as shown in Fig. 3. As for $LaMn_2Ge_2$, these results indicate the occurrence of a helical component with a propagation vector direction along the *c* axis, the extinction rules implying that the corresponding Mn moment components are antiferromagnetically coupled within the (001) planes.

(ii) At room temperature, the patterns of $PrMn_2Ge_2$ and $NdMn_2Ge_2$ exhibit magnetic contributions for nuclear lines (*hkl*) with $h + k = 2n + 1$. This is particularly obvious for the (101) line for which the observed intensity is much greater than the purely nuclear calculated intensity. As for $LaMn_2Si_2$, this result indicates an anti-C ordering, giving evidence of an antiferromagnetic arrangement of an Mn moment component within the (001) planes.

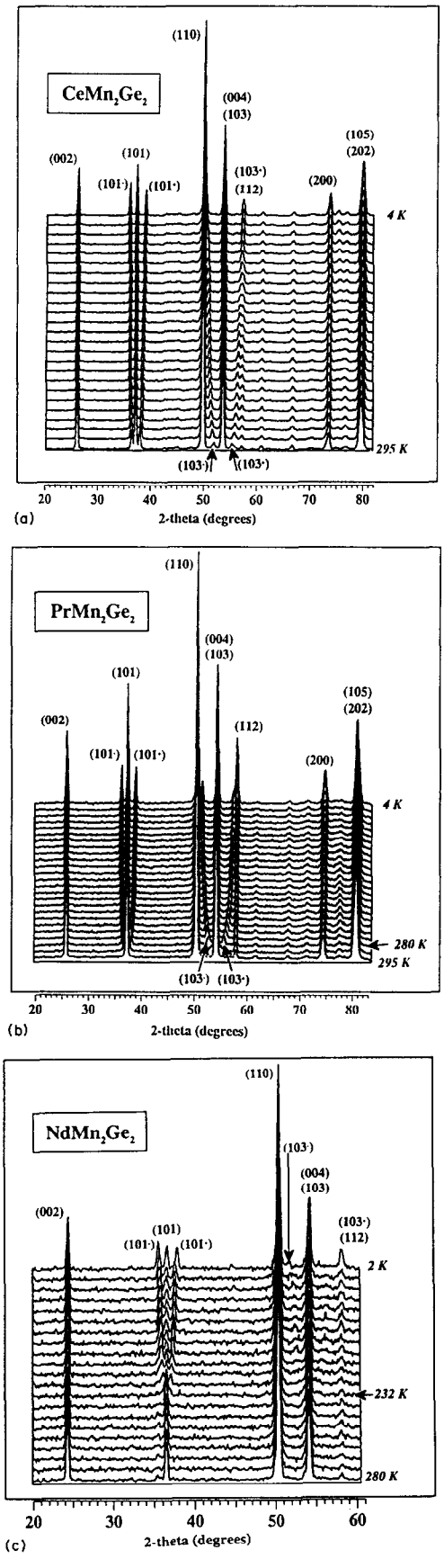

Fig. 2. Neutron thermograms of $CeMn_2Ge_2$, $PrMn_2Ge_2$ and $NdMn_2Ge_2$ recorded between 300 and 4 K.

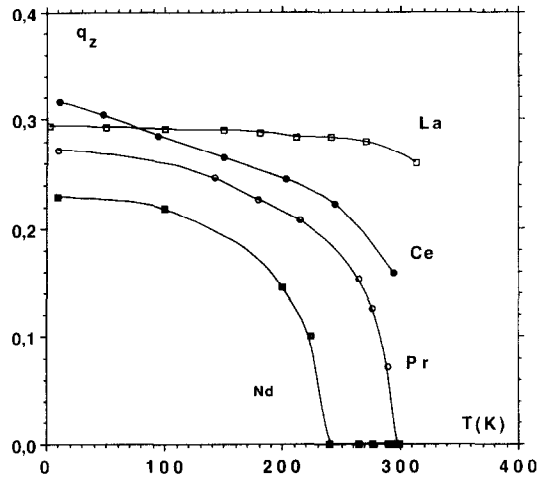

Fig. 3. Temperature dependence of the q_z component of the wavevector in the RMn_2Ge_2 (R = La, Ce, Pr, Nd) compounds.

(iii) All the thermograms are characterized by the occurrence of magnetic contributions for nuclear peaks (*hkl*) with $h+k=2n$. This is particularly obvious for the (112) line for which the nuclear contribution has an almost-zero net value. This implies that, in the whole temperature range, an additional ferromagnetic component occurs on the Mn sublattice.

From these observations, one can conclude that, in RMn_2Ge_2 (R = Ce–Nd), the Mn sublattice exhibits either a canted ferromagnetic arrangement (as in $LaMn_2Si_2$) or a conical arrangement (as in $LaMn_2Ge_2$). The thermal variations in the characteristic reflections previously defined then allow the domain of stability of each magnetic arrangement to be determined. In addition, depending on the easy axis direction and on the value of the Mn moment, each compound exhibits its own relative intensities and thermal variations of the magnetic contributions. Moreover, it noteworthy that, at low temperature, the magnetic contributions due to the ordering of the rare earth sublattice have to be considered.

A careful analysis of the neutron diffraction patterns is now necessary to clarify these points.

4.1. $CeMn_2Ge_2$

Neutron diffraction patterns recorded at 300 and 2 K are shown in Fig. 4. They are essentially characterized by the occurrence of the two satellites $(101)^+$ and $(101)^-$ with very large intensities. It is rather surprising than these reflections were not detected by Leciejewicz et al. [16]. Moreover, it is noteworthy that these researchers do not present any diffraction patterns in their publication.

The thermal variations in the intensities of the (002), (101), $(101)^-$ and (112) reflections are shown in Fig. 4. There is no evidence of significant change in the (101) and (002) line intensities which are purely nuclear. These observations imply that (i) in the whole studied temperature range, the in-plane antiferromagnetic Mn component is quenched into the incommensurate part, (ii) the Ce sublattice does not order at low temperature, at least above 2 K, and (iii) the ferromagnetic component is along the *c* axis. Moreover, the (112) and $(101)^-$ line intensities increase when the temperature decreases following the thermal variation in the ferromagnetic and incommensurate Mn moment components.

Under these conditions, the magnetic structure is conical (Fig. 5) which forms a serious revision of the previous data in Ref. [16]. At 2 K, the best refinement leads to $2.25(4)\mu_B$ and $1.5(2)\mu_B$ for the helical and ferromagnetic components respectively, yielding a cone semiangle α of approximately 56° (Table 2). The total resulting Mn moment of about $2.7\mu_B$ is much higher than that found by magnetization measurements (Table 1) and in a previous neutron diffraction study [16].

Table 2 gives the observed and calculated intensities together with the lattice constants and the various adjustable parameters at 300 and 2 K.

4.2. $PrMn_2Ge_2$

Neutron diffraction patterns recorded at 295, 142 and 2 K together with the thermal variation in the

Table 2
Calculated and observed intensities, lattice constants and adjustable parameters in $CeMn_2Ge_2$ at 300 and 2 K

hkl	300 K		2 K	
	I_c	I_0	I_c	I_0
002	64.1	63.0(6)	62.2	60.6(6)
101^-	39.4	41.6(8)	55.7	68.9(9)
101	97.8	117(1)	102.2	114(1)
101^+	41.1	43.4(9)	60.5	60.4(9)
110	776.5	753(5)	869.5	845(15)
103^-	33.6	29(1)	46.8	41(1)
103				
004	412.9	429(4)	449.1	454(5)
103^+	32.9	28(1)		
112	10.9	13(1)	93.9	97(2)
200	180.1	163(6)	210.6	223(3)
114	19.8	25(2)	28.1	35(3)
105^-		14(2)	34.3	50(3)
105				
202	772.9	741(6)	782.3	772(17)
a (Å)		4.147(1)	4.1301(9)	
c (Å)		10.946(3)	10.915(5)	
f_{cor}		1.10(2)	1.11(1)	
z_{Ge}		0.385(2)	0.383(1)	
q_z		0.159(1)	0.317(1)	
μ_{Mn} (μ_B)		2.08	2.70	
μ_{Mn} (μ_B) (F)		0.75(39)	1.52(25)	
μ_{Mn} (μ_B) (AF)		1.94(9)	2.25(4)	
R (%)		4.7	3.3	

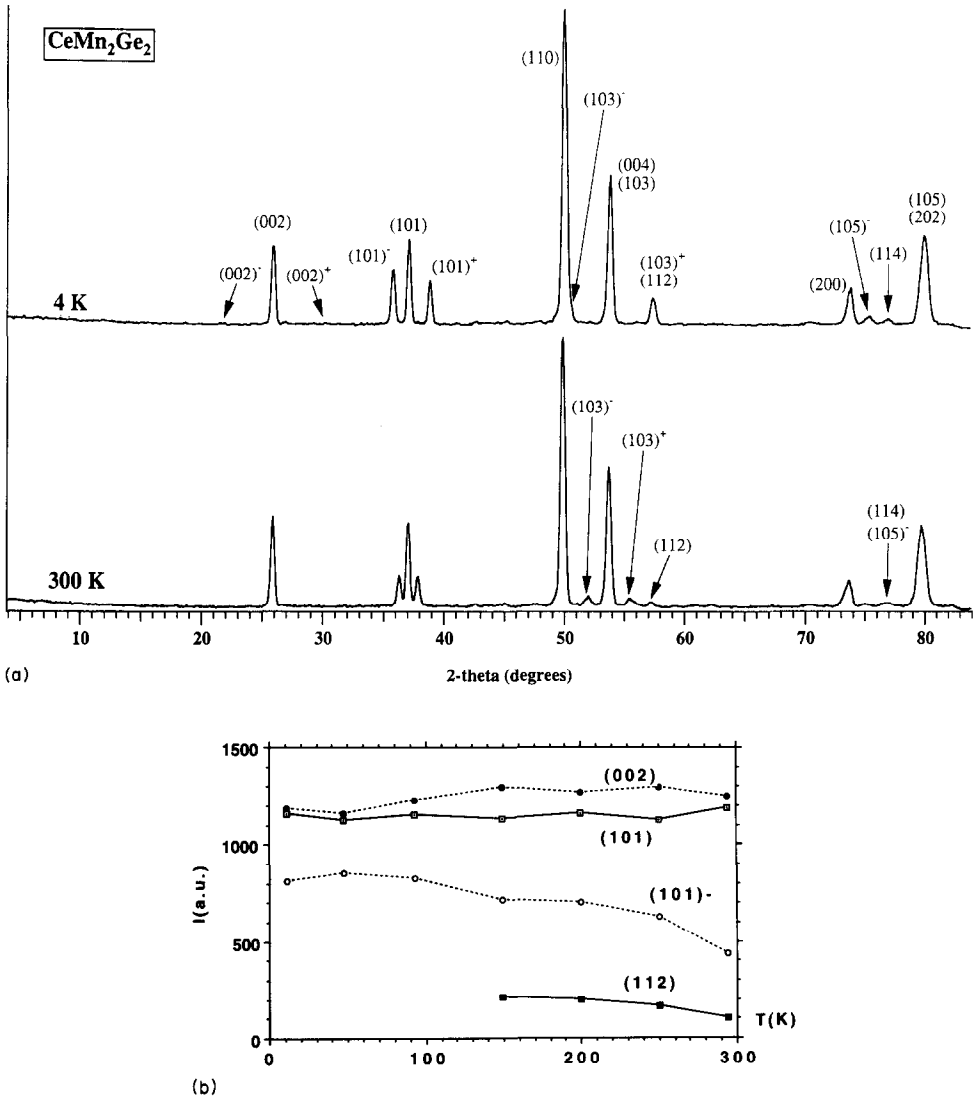

Fig. 4. (a) Neutron diffraction patterns of $CeMn_2Ge_2$ at 300 and 2 K and (b) temperature dependence of the (002), (101), $(101)^-$ and (112) characteristic line intensities. (Below about 150 K, the (112) line intensity is convoluted with the $(103)^+$ line; see the patterns.)

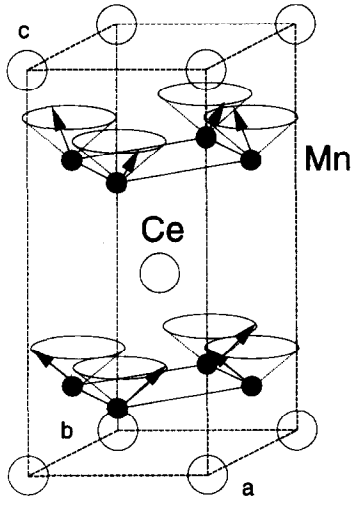

Fig. 5. Magnetic structure of $CeMn_2Ge_2$ in the whole temperature range 300–2 K.

intensities of the (002), (101), $(101)^-$ and (112) reflections are presented in Fig. 6. As for $CeMn_2Ge_2$, the (002) line intensity remains constant in the whole temperature range 2–295 K, indicating that the ferromagnetic components of the moments are aligned along the c axis, in good accordance with the previous single-crystal magnetic measurement of Iwata et al. [14]. According to the thermal variation in the intensities of the other reflections, three steps have to be considered.

At 295 K, in agreement with the observed magnetic contributions, the refinements were performed to account for the canted ferromagnetic structure sketched in Fig. 7 (see above and Section 4.2.2. of Ref. [17]). The antiferromagnetic component (about $2.2\mu_B$) lies in the (001) plane whereas the ferromagnetic component (about $1\mu_B$) is parallel to the c axis. The canting angle ϕ from the c axis is about 65° and the total resulting

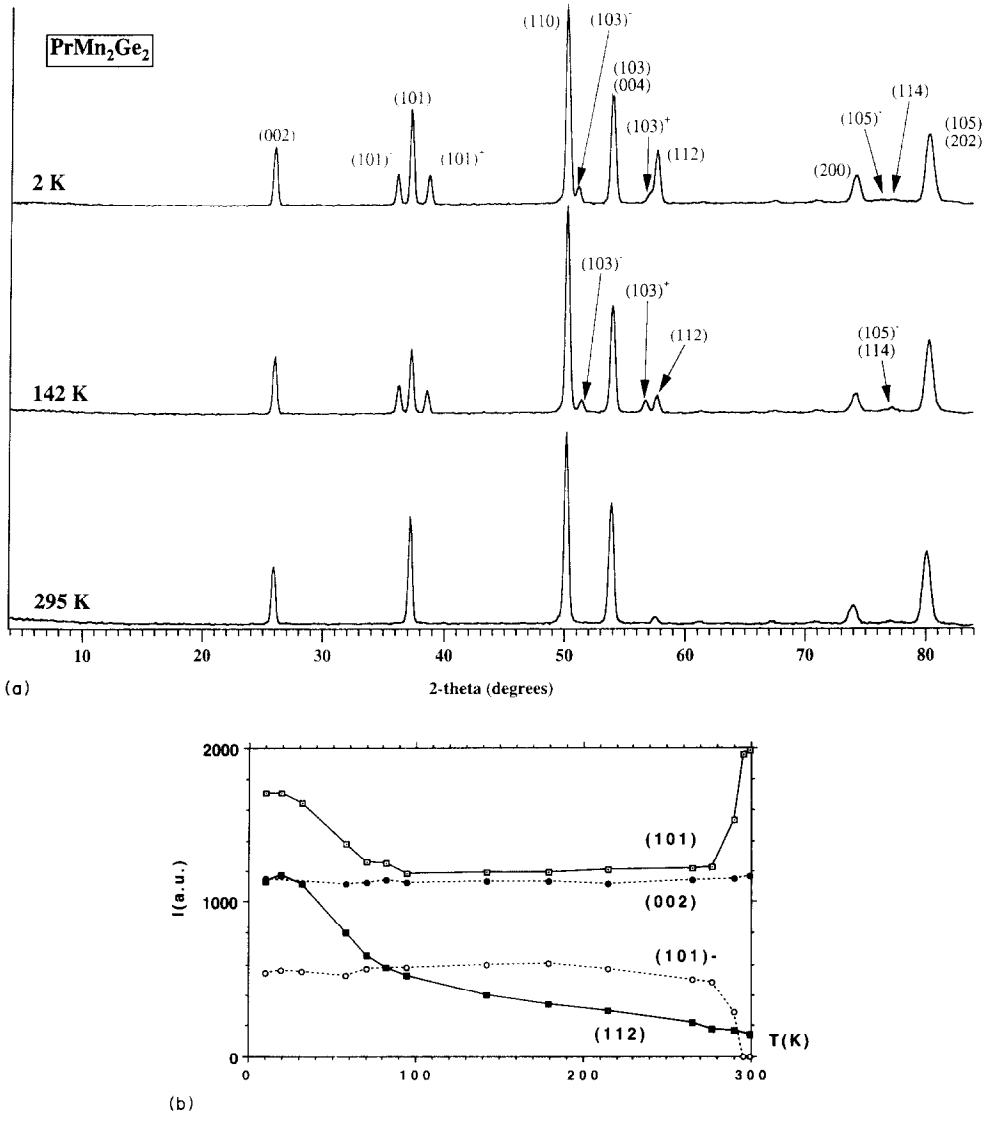

Fig. 6. (a) Neutron diffraction patterns of $PrMn_2Ge_2$ at 295, 142 and 2 K and (b) temperature dependence of the (002), (101), $(101)^-$ and (112) characteristic line intensities.

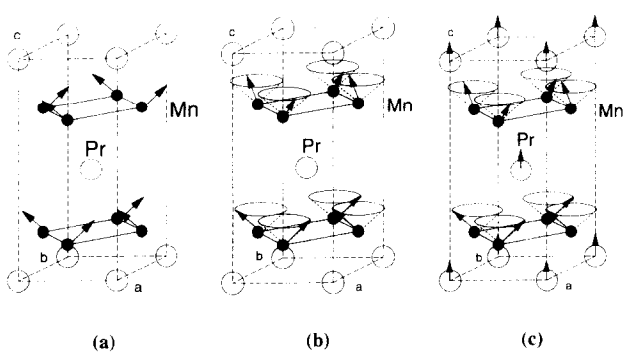

Fig. 7. Magnetic structures of $PrMn_2Ge_2$ at (a) 295 K, (b) 142 and (c) 2 K.

Mn moment μ_{Mn} is found to be about $2.4\mu_B$ per atom (Table 3).

Below about 280 K, the magnetic contribution to the (101) line intensity strongly decreases simultaneously with the rise of the satellite reflections previously defined. Under these conditions the patterns are quite similar to those observed for $CeMn_2Ge_2$, yielding the same ordering of the Mn sublattice (Fig. 7). At 142 K, the refinements yield a cone semiangle α of approximately 58° (Table 3). However, it should be noticed that best refinements need to take into account a ferromagnetic ordering of the Pr sublattice with a moment value of about $1\mu_B$ (see below).

Below about 100 K, strong increases in the (101) and (112) line intensities are observed. Evidence of ferromagnetic ordering of the praseodymium sublattice is clearly obtained from the growth of the (101) peak, since, owing to the special position of manganese (see Section 2), ferromagnetic ordering of the Mn sublattice cannot contribute to this peak. Furthermore, the absence of magnetic (00*l*) contributions leads to alignment of the Pr moments along the *c* axis. The magnetic structure

Table 3
Calculated and observed intensities, lattice constants and adjustable parameters in $PrMn_2Ge_2$ at 295, 142 and 2 K

hkl	295 K		142 K		2 K	
	I_c	I_0	I_c	I_0	I_c	I_0
002	34.8	34.5(4)	34.2	33.6(4)	34.9	34.3(4)
101⁻	–	–	29.7	32.0(5)	31.5	29.4(4)
101	114.8	114.7(9)	68.5	68.4(9)	97.9	97.8(9)
101⁺	–	–	31.8	27.1(6)	33.7	34.7(6)
110	383.2	382(2)	411.6	411(2)	390.9	391(2)
103⁻	–	–	27.5	27.4(8)	30.1	36(1)
103						
004	316.6	317(2)	273.1	274(4)	280.0	279(3)
103⁺	–	–	26.1	32(1)	28.4	29(1)
112	17.0	17.0(8)	47.6	47(1)	139.4	139(1)
200	89.8	110(4)	116.2	121(2)	160.4	167(3)
105⁻	–	–			18.8	14(2)
114	19.6	15(2)	33.4	25(2)	14.9	15(2)
105						
202	450.3	460(8)	409.8	429(9)	418.9	439(8)
a (Å)		4.123(1)		4.116(1)		4.113(1)
c (Å)		10.925(3)		10.902(4)		10.896(4)
f_{cor}		1.04(1)		1.06(1)		1.05(1)
z_{Ge}		0.381(1)		0.381(1)		0.381(1)
q_z		0		0.241(1)		0.268(1)
μ_{Mn} (μ_B)		2.4		2.8		2.8
μ_{Pr} (μ_B)		0		1.00(30)		2.95(20)
μ_{Mn} (μ_B) (F)		1.05(3)		1.41(40)		1.48(25)
μ_{Mn} (μ_B) (AF)		2.19(15)		2.40(10)		2.40(10)
R (%)		3.3		3.4		3.2

is shown in Fig. 7. At 2 K, $\mu_{Pr} \approx 2.9\mu_B$. The conical arrangement of the Mn sublattice remains with a cone semiangle α of approximately 58° (Table 3) and a resulting Mn moment of about $2.8\mu_B$. Under these conditions, a total moment of about $8.5\mu_B$ is obtained.

Table 3 gives the observed and calculated intensities together with the lattice constants and the various adjustable parameters at 295, 142 and 2 K.

4.3. $NdMn_2Ge_2$

Neutron diffraction patterns recorded at 287, 150 and 2 K are shown in Fig. 8 together with the thermal variation in the four characteristic reflections. Except for the (002) line, all the data are similar to those obtained for the Pr compound yielding the same magnetic arrangements. Here again, three steps are to be considered.

Above about 250 K, an easy axis canted ferromagnetic structure occurs (Fig. 9). The canting angle α from the c axis is about 58° and the total resulting Mn moment μ_{Mn} is found to be $1.8\mu_B$ per atom (Table 4).

At about 250 K, a conical magnetic ordering of the Mn sublattice is stabilized. Nevertheless, in agreement with the increase in the (002) line intensity, the best refinements lead us to place the easy axis direction in the (001) plane, in good accordance with the spin flop process observed in our bulk magnetic measurements and those that Shigeoka et al. performed on single crystals [13]. The magnetic structure is shown in Fig. 9. At 150 K, the refinements yield a cone semiangle α of approximately 58° (Table 4). Furthermore, in this case, no contribution from the Nd sublattice is detected at this temperature.

Below about 100 K, the strong increase in the (101) and (112) lines evidences a ferromagnetic ordering of the neodymium sublattice. The slight decrease in the (002) line is also related to the Nd moment ordering since, owing to the atomic positions of Mn and Nd atoms (see Section 2), the magnetic structure factor of this line is given by the difference between the magnetizations of the Mn and Nd sublattices. The best refinements lead to the magnetic structure shown in Fig. 9. At 2 K, the conical arrangement of the Mn sublattice remains with a cone semiangle α of approximately 56° and a resulting total Mn moment of about $2.7\mu_B$ while $\mu_{Nd} \approx 2.3\mu_B$. The ferromagnetic component of the manganese moment and the Nd moments remain in the (001) plane and are ferromagnetically coupled to each other, giving rise to a total magnetization of about $7.7\mu_B$.

Table 4 gives the observed and calculated intensities together with the lattice constants and the various adjustable parameters at 287, 150 and 2 K.

4.4. Remarks

Because of lack of independent magnetic data and because of the strong texture effects (f_{cor}), it is rather difficult to refine accurately the values of the ferromagnetic components occurring on the Mn and rare earth sublattices. These observations explain the relatively poor accuracy obtained for these moment amplitudes, particularly in the intermediate temperature ranges. Nevertheless, one can assume that the total Mn moment values are always greater than those deduced from magnetic measurements which seem only to "follow" the ferromagnetic component behaviours. New neutron diffraction experiments performed (i) in the paramagnetic state (scale factor) or (ii) on powder samples at a shorter wavelength (i.e. 1.34 against 2.5 Å) and/or on single crystals would be necessary to confirm this point. They are in progress.

Secondly, it is noteworthy that, in all the RMn_2Ge_2 (R = Ce – Nd) compounds studied in this paper, the value of the ferromagnetic component strongly decreases between 2 K and room temperature and probably vanishes at T_c while the value of the helimagnetic component decreases slightly in the same temperature range (Tables 2–4). As observed for $LaMn_2Ge_2$ [17], these results clearly suggest that an ordering temperature T_N, not detected by bulk susceptibility measure-

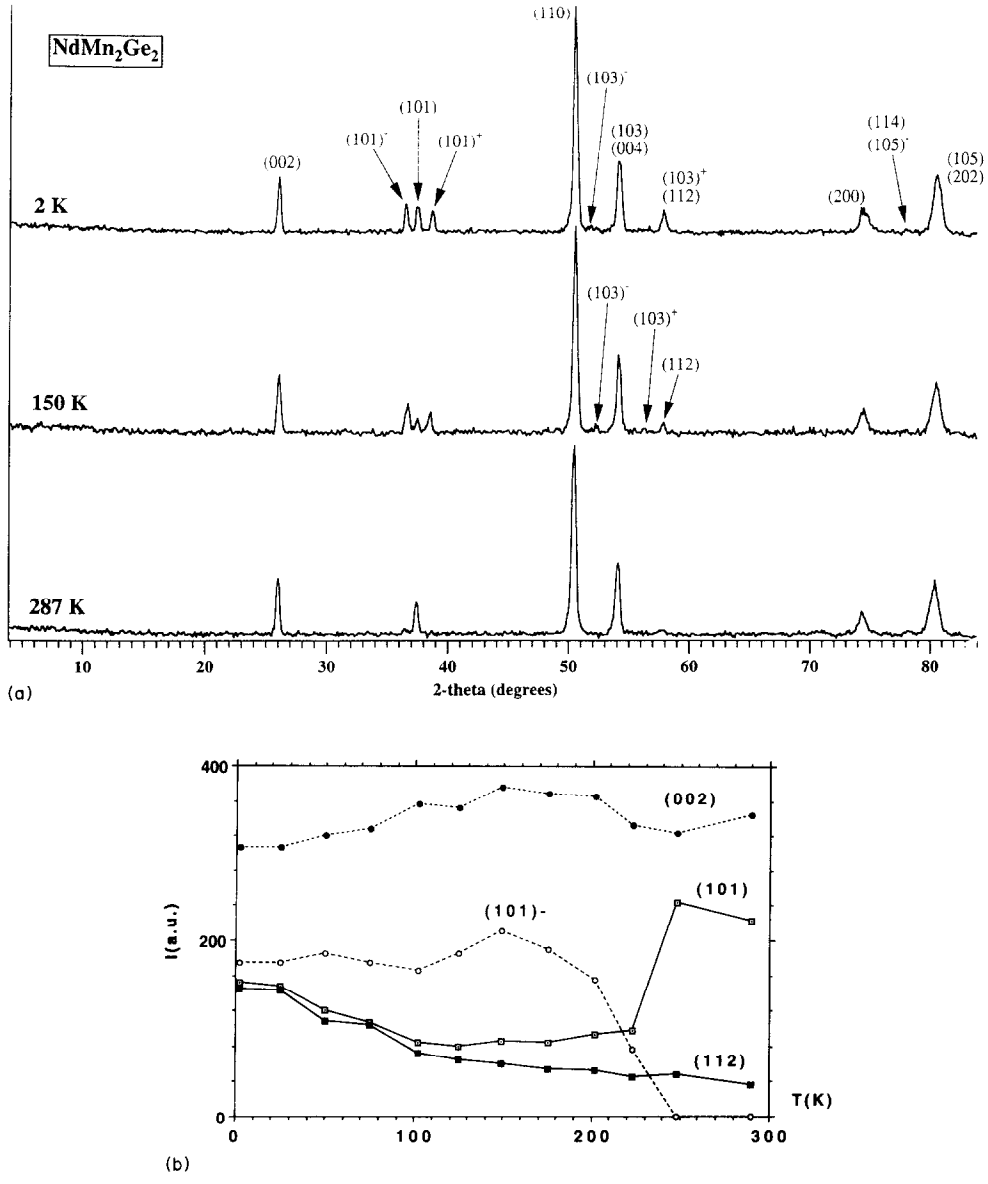

Fig. 8. (a) Neutron diffraction patterns of $NdMn_2Ge_2$ at 287, 150 and 2 K and (b) temperature dependence of the (002), (101), $(101)^-$ and (112) characteristic line intensities.

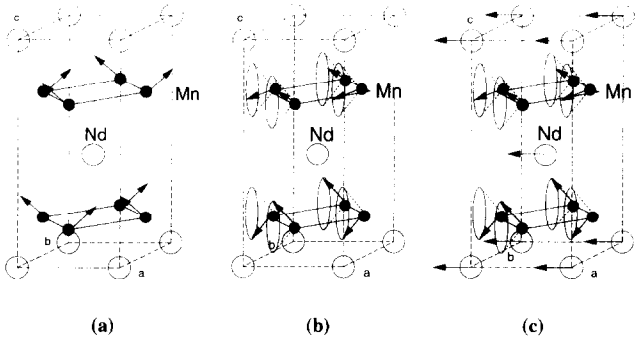

Fig. 9. Magnetic structures of $NdMn_2Ge_2$ at (a) 287 K, (b) 150 K and (c) 2 K.

ments, must occur at temperatures much higher than the Curie point. A neutron diffraction study above room temperature will be helpful to characterize this hypothetical magnetic ordering and to give an estimate of T_N. According to the data of Nowick et al. [21], the T_N values would be in the temperature range from 395 K ($SmMn_2Ge_2$) to 420 K ($LaMn_2Ge_2$).

5. Discussion

According to the collinear ferromagnetic structure of $CeMn_2Ge_2$ proposed by Leciejewicz et al. [16], the light rare earth RMn_2Ge_2 (R = La–Nd) compounds can be described and analysed as pure ferromagnets. The

Table 4
Calculated and observed intensities, lattice constants and adjustable parameters in $NdMn_2Ge_2$ at 287, 150 and 2 K

hkl	287 K		150 K		2 K	
	I_c	I_0	I_c	I_0	I_c	I_0
002	17.6	17.8(4)	19.7	19.3(8)	16.4	15.8(4)
101⁻	0	–	17.5	20(1)	16.0	16.2(6)
101	22.4	22.4(6)	9.4	9(1)	15.1	14.6(6)
101⁺	0	–	16.5	15(1)	15.1	14.6(7)
110	239.1	238(3)	244.5	242(5)	247.9	248(3)
103⁻	0	–	7.5	7(1)	6.4	6.6(8)
103						
004	107.0	107(2)	102.6	104(4)	108.3	108(2)
103⁺	0	–	6.9	5(1)		
112	6.8	6.7(8)	8.5	11(2)	29.3	31(2)
200	66.9	71(2)	68.4	76(7)	79.5	81(4)
114	1.3	0				
105⁻	–		8.1	4(3)	3.7	6(2)
105						
202	216.8	215(4)	207.6	215(9)	197.2	216(7)
a (Å)		4.110(1)		4.109(1)		4.103(1)
c (Å)		10.928(6)		10.924(7)		10.901(4)
f_{cor}		1.18(1)		1.19(2)		1.22(1)
z_{Ge}		0.387(1)		0.386(2)		0.386(1)
q_z		0		0.183(2)		0.227(1)
μ_{Mn} (μ_B)		1.8		2.7		2.7
μ_{Nd} (μ_B)						2.35(24)
μ_{Mn} (μ_B) (F)		0.97(21)		1.48(29)		1.52(24)
μ_{Mn} (μ_B) (AF)		1.59(10)		2.27(12)		2.26(9)
R (%)		1.4		3.5		5.3

present study gives evidence of large antiferromagnetic components within the (001) Mn planes in the whole RMn_2Ge_2 (R = La–Nd) series and leads us to revise strongly the conclusions deduced from this previous description.

In the whole temperature range 300–2 K, $CeMn_2Ge_2$ exhibits a conical magnetic structure (semicone angle $\alpha \approx 60°$). The same Mn sublattice behaviour is encountered for $PrMn_2Ge_2$ and $NdMn_2Ge_2$, at least below about 250 K. For the three compounds, the helical turn angle between adjacent Mn layers increases when decreasing the temperature as well as when going from Nd to Ce compounds (from 40° to 57° at 2 K). For such an α value (about 60°), in the whole temperature range 2–300 K, the antiferromagnetic component is greater than the ferromagnetic component. At low temperature, the praseodymium and neodymium moments are ferromagnetically coupled with the ferromagnetic component of the manganese moment, in good accordance with the general behaviour of the light rare earth–(3d) transition metal exchange. Moreover, both $CeMn_2Ge_2$ and $PrMn_2Ge_2$ compounds (and $NdMn_2Ge_2$ at room temperature) exhibit an easy axis anisotropy whereas an easy plane occurs in $NdMn_2Ge_2$ below 250 K.

In spite of some uncertainties concerning the refined parameters (see Section 4.4), the moment values deduced from the neutron diffraction data are now in agreement with those observed previously in such compounds [17,24,30,31]. In all RMn_2Ge_2 (R = La–Nd) compounds, the reduced Mn moment values deduced from all the magnetization measurements (see Sections 1 and 2) clearly correspond to the purely ferromagnetic components of their magnetic structures, the antiferromagnetic component being obscured at least below $H_{appl.} = 5$ T [12–14]. Furthermore, it should be noticed that the Nd and Pr moment values, assumed by Shigeoka et al. [13] and Iwata et al. [14] in their calculations, are close to those found in the present work. This result probably explains the reasonable agreement obtained by these researchers between their calculated and experimental data.

On the contrary, the total Mn moments, deduced from the present study, account well for the hyperfine values obtained by Sampathkumaran et al. [22] from ^{55}Mn NMR experiments. Moreover, according to the occurrence of an incommensurate magnetic component in these compounds, the apparent crystallographic disorder noted by these workers in their NMR spectra probably originates from a distribution of Mn sites due to the different orientations of the hyperfine fields with respect to the principal axis of the electric field gradient.

Until now, all the known magnetic structures of $ThCr_2Si_2$-type manganese silicides and germanides were said to be characterized by ferromagnetic (001) Mn planes, stacked ferro- or antiferromagnetically along the c axis (for a long review, see Ref. [32]). The correctness of the conclusions deduced from this observation (i.e. the correlation between the lattice constants and the Mn sublattice ordering) has been largely discussed in a previous paper [17]. From the present work and Ref. [17], it is now obvious that all the RMn_2X_2 compounds which behave ferromagnetically are characterized by a dominant antiferromagnetic component in the (001) plane whereas those which behave antiferromagnetically, such as $PrMn_2Si_2$ [24] and $DyMn_2Ge_2$ [31] for example, exhibit purely ferromagnetic Mn planes; therefore, it seems that both phenomena might be correlated. The origin of this particular behaviour has already been discussed in Ref. [17] and is actually unknown. Nevertheless, some correlations clearly appear in the plots presented in Fig. 10, to be discussed below.

In Fig. 10(a), the Mn moment values are plotted as a function of the contraction of the Mn–X (X = Si, Ge) distance from the sum of the elemental radii (given by E. Teatum, K. Gschneider and J. Waber in 1960, cited in Ref. [32]) for the related series RMn_2Ge_2 in this work and Refs. 17,20,31,33], RMn_2Si_2 [17,23,24,33], RMnGe [19], RMnSi [18] and $RMnSi_2$ [30]. It clearly appears that the Mn moment values have to be cor-

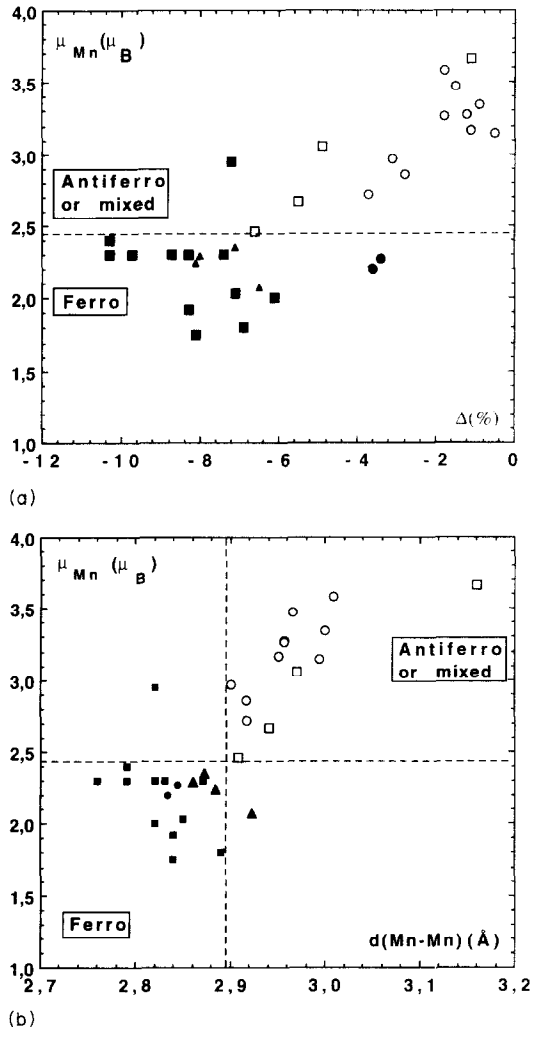

Fig. 10. Plot of the Mn moment values vs. (a) the relative contraction of the Mn–X distances d (X = Si, Ge) from the sum of the elemental radii [32] (Δ (%) = $100(d-\Sigma r)/\Sigma r$) and (b) the Mn–Mn intralayer separation (structure types: □, ■, $ThCr_2Si_2$; ○, ●, CeFeSi; ▲, $TbFeSi_2$).

related with the Mn–X distance, i.e. a strong contraction leads to a low value of μ_{Mn} and vice versa. This behaviour has been discussed at length in Refs. [17] and [18]. Moreover, Fig. 10(a) also shows that the compounds with a large Mn moment are characterized by antiferromagnetic or mixed (ferro- and antiferromagnetic components) Mn planes. Both ranges are clearly separated by the critical value $\mu_{Mn} \approx 2.5\mu_B$.

On the contrary, as the Mn–Mn distance is strongly related to the Mn–X distances, the same correlations appear in Fig. 10(b) where the Mn moment values are plotted as a function of the Mn–Mn intralayer separation. This figure clearly shows that antiferromagnetic Mn planes occur in compounds characterized by large Mn–Mn intralayer distances d_{ip} (see Section 1) whereas ferromagnetic Mn planes occur in compounds characterized by small Mn–Mn distances. It is noteworthy that the critical Mn–Mn intralayer distance is about 2.87 Å, a value close to those defined by Welter and co-workers in the CeFeSi-type RMnX compounds [18,19]. We have already discussed this criterion in Refs. [17,19,30] and a long review can be found in Ref. [35]. Furthermore, in the latter paper, Kaneko et al. [35] note that, in Cu_2Sb-type ternary compounds (MnMX where M = Al, Ga, Zn, Ca and X = Ge, Sb), the Mn moment value is large (about $4\mu_B$) when the Mn–Mn separation is greater than 2.85 Å and low (about $2\mu_B$) when the Mn–Mn separation is less than 2.85 Å. All these observations suggest that there is a certain critical Mn–Mn distance where the Mn magnetic properties change drastically. It is noteworthy that Szytula and Siek [36] have, for the first time, used the same criterion in order to explain the interplane coupling, i.e. assuming purely ferromagnetic Mn planes, intralayer Mn–Mn distances greater than 2.86 Å lead to ferromagnetic interplane coupling, whereas distances lower than 2.86 Å lead to antiferromagnetic interplane interactions.

In fact, the interlayer interactions appear to be very complicated. One may think that antiferromagnetic (001) Mn planes induce additional interplane ferromagnetic interactions which begin to act when the thermal contraction of the lattice constants smoothes the in-plane interactions. Moreover, the strength of these additional interactions seems to be very sensitive to the electron concentrations. In the alkaline earth germanides $CaMn_2Ge_2$ and $BaMn_2Ge_2$ [20], the Mn planes are purely antiferromagnetic while antiferromagnetic and ferromagnetic components occur within the Mn planes in the RMn_2Ge_2 (R = La–Nd) and $LaMn_2Si_2$ compounds. Assuming that large Mn–Mn separations ($d > 2.85$ Å) lead to antiferromagnetic (001) Mn planes, the canted magnetic structures observed in the large-sized rare earth manganese silicides and germanides may arise as a result of strong ferromagnetic interplane interactions which would tend to align the Mn moments in each (001) plane. Moreover, the interplane interactions also affect the antiferromagnetic component couplings, yielding commensurate or incommensurate behaviour. Fig. 3 clearly shows the evolution of the wavevector with the size of the rare earth. The cerium compound slightly differs from the other compounds. Here again, the different electronic state of this element probably accounts for this effect. Finally, we must remember that these compounds seem to behave as purely collinear antiferromagnets above T_c [17,21].

6. Conclusion

Neutron diffraction studies of $CeMn_2Ge_2$, $PrMn_2Ge_2$ and $NdMn_2Ge_2$ have revealed the occurrence of a dominant antiferromagnetic component within the (001) Mn planes in these compounds previously reported as

collinear ferromagnets. Furthermore, the present study leads to more reasonable Mn moment values of about $2.5\mu_B$ against the value $1.5\mu_B$ previously published. These results clearly show that a better understanding of the magnetic properties of these compounds obviously needs the use of the neutron technique.

From the present work, we unambiguously show that all the $ThCr_2Si_2$-type RMn_2X_2 compounds which behave ferromagnetically exhibit this type of Mn sublattice magnetic arrangement. This magnetic behaviour seems to be correlated with the magnitude of the Mn moment and/or with the Mn–Mn intralayer separation. The effect of ferromagnetic and antiferromagnetic planes on the interplane couplings is less clear, although the two effects seem to be correlated.

Further investigations of the RMn_2Ge_2 (R = La–Nd) series above T_c are now necessary to complete this work. Moreover, neutron diffraction studies of solid solutions where ferromagnetic–antiferromagnetic transitions occur may provide useful information concerning the correlation between the bulk magnetic behaviour and the occurrence of antiferromagnetic Mn components. Such experiments will also allow us to examine more precisely the Mn–Mn intralayer spacing criterion. These studies are underway.

It would also be interesting to re-analyse the magnetic properties of the $SmMn_2Ge_2$ in the light of the present work. It is noteworthy that the often-studied $SmMn_2Ge_2$ compound might behave similarly and one may expect the occurrence of in-plane antiferromagnetic components when this compound behaves ferromagnetically and purely ferromagnetic Mn planes when it becomes antiferromagnetic at lower temperature. Because of the too-large absorption coefficient of Sm, a neutron diffraction study of the $La_xY_{1-x}Mn_2Ge_2$, $Nd_xY_{1-x}Mn_2Ge_2$ or $La_xNd_{1-x}Mn_2Si_2$ solid solutions where the x values were chosen to yield an $SmMn_2Ge_2$-like behaviour has been done and results will be published elsewhere [37].

References

[1] K.S.V.L. Narashimhan, V.U.S. Rao, W.E. Wallace and I. Pop, *AIP Conf. Proc., 29* (1976) 594.

[2] W. Dörrscheidt, N. Niess and H. Schäfer, *Z. Naturforsch. B, 31* (1976) 890.

[3] K.S.V.L. Narashimhan, V.U.S. Rao, R.L. Bergner and W.E. Wallace, *J. Appl. Phys., 46* (11) (1975) 4957.

[4] A. Szytula and I. Szott, *Solidi State Commun., 40* (1981) 199.

[5] H. Fujii, T. Okamoto, T. Shigeoka and N. Iwata, *Solid State Commun., 53* (8) (1985) 715.

[6] M. Duraj, R. Duraj, A. Szytula and Z. Tomkowitz, *J. Magn. Magn. Mater., 73* (1988) 240.

[7] M. Duraj, R. Duraj and A. Szytula, *J. Magn. Magn. Mater., 79* (1989) 61.

[8] M. Slaski, T. Laegrid, K. Fossheim, Z. Tomkowicz and A. Szytula, *J. Alloys Comp., 178* (1992) 249.

[9] P. Hill and N. Ali, *J. Appl. Phys., 73* (10) (1993) 5683.

[10] M.P. Pugacheva and Z. Onyszkiewicz, *Phys. Status Solidi B, 177* (1993) K89.

[11] R.B. van Dover, E.M. Gyorgy, R.J. Cava, J.J. Krajewski, R.J. Felner and W.F. Peck, *Phys. Rev. B, 47* (10) (1993) 6134.

[12] T. Shigeoka, N. Iwata, J. Fujii and T. Okamoto, *J. Magn. Magn. Mater., 53* (1985) 83.

[13] T. Shigeoka, N. Iwata and H. Fujii, *J. Magn. Magn. Mater., 76–77* (1988) 189.

[14] N. Iwata, T. Ikeda, T. Shigeoka, H. Fujii and T. Okamoto, *J. Magn. Magn. Mater., 54–57*(1986) 481.

[15] T. Kawashima, T. Kanomata, H. Yoshida and T. Kaneko, *J. Magn. Magn. Mater., 90–91* (1990) 721.

[16] J. Leciejewicz, A. Szytula, W. Bazela and S. Siek, *J. Magn. Mang. Mater., 89* (1990) 29.

[17] G. Venturini, R. Welter, B. Malaman and E. Ressouche, *J. Alloys Comp., 210* (1994) 213.

[18] R. Welter, G. Venturini and B. Malaman, *J. Alloys Comp., 206* (1994) 55.

[19] R. Welter, *Thesis,* Université de Nancy I, 1994.

[20] B. Malaman, G. Venturini, R. Welter and E. Ressouche, *J. Alloys Comp., 210* (1994) 209.

[21] I. Nowick, Y. Levi, I. Felner and E.R. Baussinger, *J. Magn. Magn. Mater.,* (1994) in press.

[22] E.V. Sampathkumaran, L.C. Gupta, R. Vijayaraghavan, Le Dang Khoi and P. Veillet, *J. Phys. F, 12* (1982) 1039.

[23] S. Siek, A. Szytula and J. Lieciejewicz, *Phys. Status Solidi A, 46* (1978) K101.

[24] R. Welter, G. Venturini, D. Fruchart and B. Malaman, *J. Alloys Comp., 191* (1993) 263.

[25] D. Rossi, R. Marazza, D. Mazzone and R. Ferro, *J. Less-Common Met., 59* (1978) 79.

[26] R. Welter, G. Venturini and B. Malaman, *J. Alloys Comp., 189* (1992) 49.

[27] C. Stassis, H.W. Deckman, B.N. Harman, J.P. Desclaux and A.J. Freeman, *Phys. Rev. B, 15* (1977) 369.

[28] C.G. Shull and Y. Yamada, *J. Phys. Soc. Jpn., 22* (1962) 1210.

[29] P. Wolfers, *J. Appl. Crystallogr., 23* (1990) 554.

[30] B. Malaman, G. Venturini, L. Pontonnier and D. Fruchart, *J. Magn. Magn. Mater., 86* (1990) 349.

[31] G. Venturini, B. Malaman, K. Tomala, A. Szytula and J.P. Sanchez, *Phys. Rev. B, 46* (1) (1992) 207.

[32] W.B. Pearson, *The Crystal Chemistry and Physics of Metals and Alloys,* Wiley, New York, 1972, p. 151.

[33] A. Szytula and J. Leciejewicz, Magnetic properties of ternary intermetallic compounds of the RT_2X_2 type, *Handbook on the Physics and Chemistry of Rare Earths,* Vol. 12, 1989, Chapter 83, p. 133.

[34] R. Welter, G. Venturini, E. Ressouche and B. Malaman, *J. Alloys Comp., 210* (1994) 273.

[35] T. Kaneko, T. Kanomata, H. Yasui, T. Shigeoka, M. Iwata and Y. Nakagawa, *J. Phys. Soc. Jpn., 61* (11) (1992) 4164.

[36] A. Szytula and S. Siek, *J. Magn. Magn. Mater., 82* (1982) 319.

[37] G. Venturini, R. Welter, B. Malaman and E. Ressouche, to be published.